Physisorption Of Rare Gases On Transition Metal Trimers: A Density Functional Study

M. Kettner, A. S. Gentleman and G.F. Metha
Department of Chemistry, The University of Adelaide, South Australia 5005, Australia

1. Introduction

Currently metal surfaces are used as heterogeneous catalysts in many industrial processes, e.g. the Haber–Bosch process (α-Iron) or the Ostwald process (Platinum/Rhodium). In order to understand the mechanistic workings behind metal surface catalysts, metal clusters were utilised as model surfaces. The interaction of the clusters with small molecules was studied so that a greater understanding of catalytic processes could be achieved.[1] Studies performed involving the interactions of small molecules with metal clusters have shown interesting results. It has been found that metal clusters display size-dependent reactivity towards small molecules. Changing the cluster composition by just one atom has been found to significantly affect the reactivity.[2] This behaviour has been attributed to significant geometric and electronic property changes that occur upon composition change. However, it was soon discovered thereafter that metal clusters are not just useful as model surfaces, but can also act as catalysts in their own right. Such studies have been performed by Heiz and co-workers who have performed the CO + NO catalytic converter reaction using MgO-supported Pd_n clusters (n<30) as catalysts at temperatures T < 150 K [3]. In addition to this, they have also performed the CO oxidation reaction at a temperature of 150K using MgO-supported Au_8 clusters as catalysts for the process.[4] In both studies, the metal clusters were found to be more efficient than their bulk-metal surface counterparts.

Since it has been discovered that metal clusters show improved catalytic properties, many studies that involve probing the geometric and electronic properties of these molecules have been performed. In most of these studies, a combination of computational simulations and experimental studies were used to obtain and verify results; inferring geometric and electronic structural information for a wide variety of metal clusters. Such information is important as it can provide insight into why some metal clusters are more catalytically active than others. Modern tools like the Free Electron Laser for Infrared experiments (FELIX) [5] in conjunction with computational work provide us with new techniques like infrared multiple photon dissociation spectroscopy (IR-MPDS) to investigate the geometric and electronic structure of metal clusters. In these experiments, rare gas atoms are attached to M_n Clusters to afford M_nRg_m clusters and through the use of IR-MPDS, an IR-Spectrum of the metal cluster is obtained. This is possible as the excitation of any vibrational mode of the M_nRg_m cluster leads to the dissociation of the rare gas atom/s from the metal cluster via resonance excitation.[6] The comparison of the experimental IR-spectrum with the calculated IR-spectrum helps to determine the structure of M_n as the physisorbed rare gas atoms are believed to have a negligible influence on the structure of M_n [7]. Fielicke et al. probed V_8, V_7 and Nb_7 clusters successfully. For Nb_n (n<5) on the other hand, no Nb_nAr_m cluster was found [6]. In this work we tried to show a computed trend for simple M_3 and M_3Rg (M = Nb, Mo, Tc, Ru, Rh, Pd, Ag; Rg = Ar, Kr,Xe) clusters, their lowest energy configuration, their far-IR-dissociation spectra and their stability. A comparison between the computed properties and the computed electron affinities as well as the ionisation potentials was carried out.

2. Computational Methods

Geometric optimisations and harmonic vibrational frequencies of each cluster were calculated using the Gaussian 03 suite of programs [11]. The calculations were carried out on Corvus (an SGI Altix XE 1300 Linux cluster). For every calculation the B3P86 density functional was used.. In combination with this density functional, every metal atom in the clusters was treated with the SDD (Stuttgart-Dresden) Basis Set, the Ar and Kr atoms were treated with the aug-cc-pVTZ basis set and the Xe atom was treated with the aug-cc-pVTZ-pp basis set.. The key difference between the aug-cc basis sets is a pseudo potential which lowers the computational costs of the Xe modelling and includes some relativistic effects. This in turn increases the efficiency and accuracy of the calculation.

3. Results

The calculations performed aimed to find the lowest energy structures for M_3 and M_3Rg clusters. For every M_3 cluster, six different starting structures were optimised at the five lowest multiplicities. The energy of the global minimum for each M_3 cluster and the corresponding lowest energy multiplicities are listed in Table 1a. The spin multiplicities and the structures (C_{2V}) of each M_3 cluster are similar to those found by Addicoat et al.[8] The only outstanding exception was for the lowest energy structure of Mo_3; which possessed a spin multiplicity of M = 7 as opposed to the M = 3 value listed in the literature. For every M_3Rg cluster, 40 different starting structures were optimised at the five lowest possible multiplicities for each M_3Rg cluster. The stabilisation energy of the M_3Rg cluster was calculated by taking the difference between the sum of individual energies of the bare M_3 cluster and the rare gas atom and the energy of the M_3Rg cluster. The stabilisation energy for every M_3Rg cluster investigated and the corresponding multiplicities for each global minimum are listed in Table 1b. Diagram 1 illustrates the trend in stabilisation energy for the various M_3Rg clusters. As observed from Tables 1a and 1b, physisorption of a rare gas does not change the spin multiplicity of the respective cluster. Also as observed in Table 1b and Diagram 1, the stability of the various M_3Rg clusters increases with increasing rare gas atom size. Interestingly enough, Diagram 1 also shows that Pd_3Rg and Tc_3Rg clusters possess lower system energies than the other M_3Rg clusters.

Metal cluster	E / h	M
Nb_3	-171.613554	2
Mo_3	-205.416087	7
Tc_3	-243.308539	6
Ru_3	-285.716503	9
Rh_3	-332.806709	4
Pd_3	-384.969976	3
Ag_3	-442.348236	2

Tab 1a: *Computed absolute energies of the M_3 clusters*

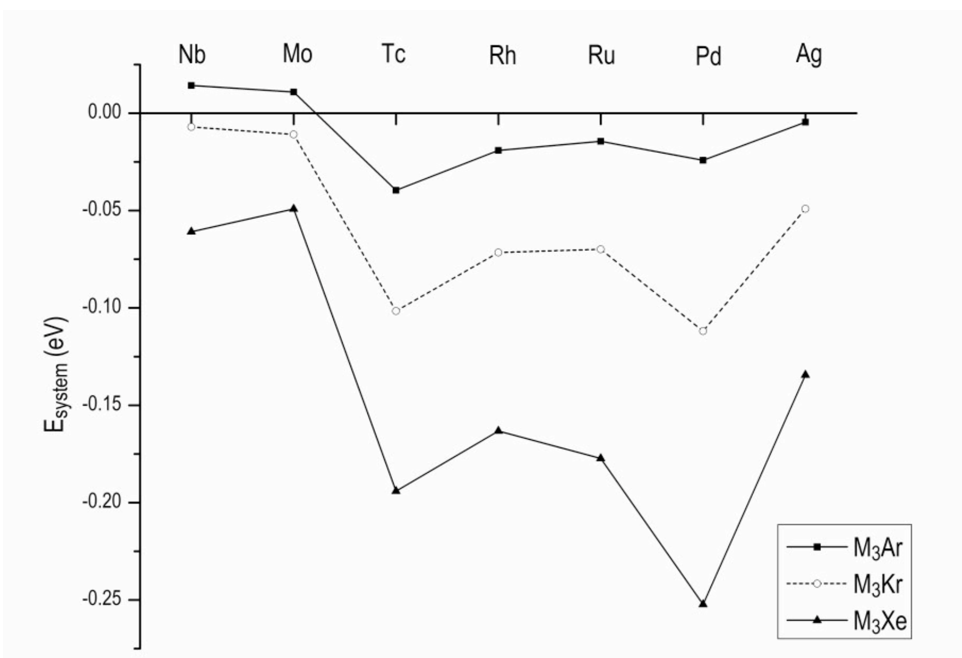

Diag.1: *Stability of M_3Rg clusters*

Element	Atomic Number	System energy / eV			Spin Multiplicity
M	*Z*	*E(M_3Ar)* / eV	*E(M_3Kr)* / eV	*E(M_3Xe)* / eV	*S*
Nb	41	0.0143	-0.0070	-0.0609	2
Mo	42	0.0109	-0.0109	-0.0492	7
Tc	43	-0.0396	-0.1016	-0.1941	6
Ru	44	-0.0191	-0.0715	-0.1632	9
Rh	45	-0.0144	-0.0699	-0.1773	4
Pd	46	-0.0242	-0.1119	-0.2523	3
Ag	47	-0.0046	-0.0491	-0.1345	2

Tab.1b: *Calculated stabilities of M_3Rg clusters and Spin Multiplicity of the lowest energy structure*

In order to investigate the observed trend in stabilisation energy of the M_3Rg clusters, the ionisation potentials (IPs) and the electron affinities (EAs) (both vertical and adiabatic) were calculated for the M_3 clusters. In doing this, some significant insight into the trend could possibly be gained as the correlation between IPs/EAs of bare metal clusters and their reactivity has been well documented [10]. The calculated IP and EA values are shown in Table 2 and Diagram 2. As observed, the highest vertical and adiabatic IP values occur for Pd_3. The highest vertical and adiabatic EA values occur for Ag_3. Overall, there was no relationship found between the IPs and EAs of the M_3 clusters and their stability. This is due to the fact that the correlation between IP/EA and reactivity only works in situations where the reactant molecule (be it a rare gas atom or small molecule) chemisorbs to the metal cluster; which involves the formation of chemical bonds. Therefore, the lack of correlation proves that the interaction between the cluster and the rare gas is not covalent and must be based on Van der Waals interactions.

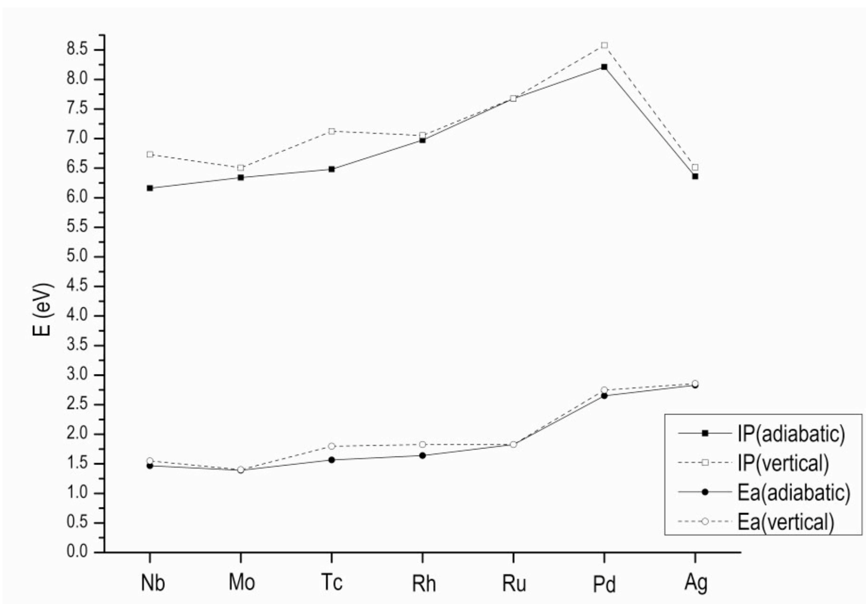

Diag. 2: *Calculated vertical and adiabatic electron affinities (EA) and ionisation potentials (IP) of M_3 clusters*

Element	*Z*	*IP(adiabatic)* / eV	*IP(vertical)* / eV	*Ea(adiabatic)* / eV	*Ea(vertical)* / eV
Nb	41	6.161	6.730	1.468	1.548
Mo	42	6.341	6.505	1.390	1.401
Tc	43	6.483	7.125	1.565	1.797
Ru	44	6.973	7.053	1.640	1.825
Rh	45	7.678	7.679	1.825	1.825
Pd	46	8.213	8.577	2.651	2.745
Ag	47	6.359	6.513	2.829	2.857

Tab.2: *Calculated vertical and adiabatic electron affinities (Ea) and ionisation potentials (IP) of M_3 clusters*

To get the direction of the dispersion interaction, the exact polarizability and the dipole moment was calculated for each M_3 cluster. Table 3 illustrates that all dipole momenta are pointing along the C_{2V} rotation axis of each trimer. This implies that the rare gas atom is expected to sit some distance from the trimer along this axis upon physisorption. Figure 1 shows that for the Mo_3Rg, Tc_3Rg, Ru_3Rg, and Ag_3Rg clusters, the rare gas atom sits at the expected place along the axis. However, this is not observed for Rh_3Rg, Pd_3Rg and Nb_3Rg. For Rh_3Rg and Pd_3Rg, the rare gas atom sits in the M_3 plane but not along the C_{2V} axis. For Nb_3Rg, the rare gas atom is situated out of the plane. Even though the absolute values of the dipole momenta show quite large variations between the different transition metal trimers, no correlation between the absolute value of the dipole moment and the stability of the M_3Rg cluster can be discovered. In addition to this, no obvious relationship between the dipole moment, polarizability and the position of the rare gas atom can be found. Clearly, further investigations are required to ascertain the factors that define where and how a rare gas atom will bind upon physisorbing to a transition metal trimer.

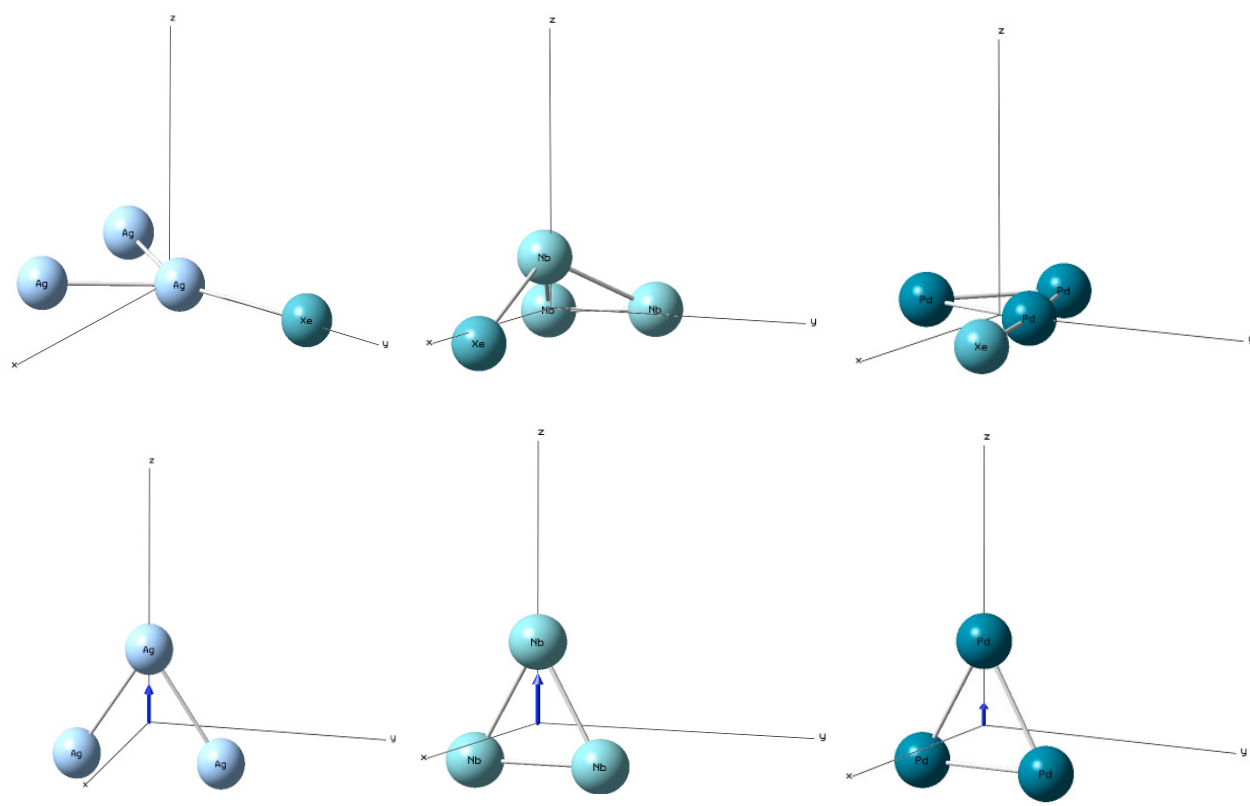

Fig. 1: *First row contains the three examples of M_3Rg clusters, second row contains M_3 clusters with the respective dipole moments (shown as arrows [not to scale])*

Element	Exact polarizability:			Dipole moment / Debey	
	lower triangular matrix			ρ_x; ρ_y; ρ_z	ρ_{Total}
Nb	156.454			0	0.4832
	0	214.834		0	
	0	0	212.458	0.4832	
Mo	140.446			0	0.2943
	0	276.5		0	
	0	0	156.39	-0.2943	
Tc	155.631			0	0.0102
	0	167.76		0	
	0	0	163.016	-0.0102	
Rh	106.999			0	0.0003
	0	145.807		0	
	0	0	145.8	-0.0003	
Ru	103.635			0	0.0411
	0	132.843		0	
	0	0	131.916	-0.0411	
Pd	87.409			0	0.0401
	0	125.575		0	
	0	0	125.678	-0.0401	
Ag	91.303			0	0.7186
	0	235.625		0	
	0	0	139.439	0.7186	

Tab. 3: *Exact polarizabilities and dipole momenta*

4. Conclusions & Future Directions

DFT investigations were performed on M_3 and M_3Rg clusters in order to gain insight in their electronic structure and stability. All our modelled M_3 clusters possessed C_{2v} symmetry, which was consistent with previous work. In addition to this, most of these metal trimers possessed the same spin multiplicity as shown in previous work. The only exception to this was the Mo_3 cluster; for which the lowest energy structure possessed a spin multiplicity of M = 7 as opposed to the M = 3 spin multiplicity described in the literature. It was found that the spin multiplicity of M_3 cluster does not change upon the physisorption of a rare gas atom.

In order to justify observed stability trends for the M_3Rg clusters, the IPs and EAs of the M_3 clusters were calculated. No direct correlation of these values and the stabilities of the M_3Rg cluster could be found. This reinforced the presumption that physisorption is the primary adsorption process for the interaction of metal clusters with rare gas atoms.

In an attempt to understand the favored binding sites of the rare gas atoms onto the M_3 clusters, the dipole momenta and the exact polarizabilities of the metal trimers were calculated. The dipole momentum of each metal trimer was found to be directed along the C_{2V} rotary axis. For some of the M_3Rg clusters, the rare gas atom was aligned along this axis upon physisorption; which was to be expected. However, for other clusters (including the most stable Pd_3Kr cluster), the rare gas atom was not aligned with this axis. No explanation could be given as to why some M_3Rg clusters have the rare gas atoms aligned along the C_{2v} axis and others do not.

Despite the fact that some insight was gained into the physisorption of rare gas atoms to metal clusters, further investigations are still required in order to explain stability trends of the M_3Rg clusters and unexpected binding sites of the rare gas atoms to some of the M_3 clusters upon physisorption. One suggestion that could be considered for future work is to perform the same calculations on the M_3 and M_3Rg clusters using density functionals that explicitly treat dispersion forces better than the B3P86 density functional. Such density functionals are still in their infancy and have not yet been incorporated in the Gaussian '03 suite of programs. Other programs such as the Amsterdam Density Functional (ADF) or GAMESS programs may have these density functionals available. However, these programs are currently not installed on Corvus and therefore cannot be used.

5. References

[1] M. E. G. M.D. Morse, J. R. Heath and R. E. Smalley J. Chem. Phys. ***1985****, 83, 2293-2304.*

[2] P. A. H. A. Bérces, Li Lian, S. A. Mitchell, and D. M. Rayner J. Chem. Phys. ***1997****, 108, 5476-5490.*

[3] S. A. Ken Judai, Anke S. Wörz, Ulrich Heiz, and Claude R. Henry J. AM. CHEM. SOC. ***2004****, 126, 2732-2737.*

[4] H. H. Bokwon Yoon, Uzi Landman, Anke S. Wörz,, S. A. Jean-Marie Antonietti, Ken Judai, and Ueli Heiz Science. ***2005****, 307, 403-407.*

[5] D. v. H. Gert von Helden, Gerard Meijer J. Phys. Chem. ***2003****, 107, 1671-1688.*

[6] G. v. H. A. Fielicke, and G. Meijer The European Physical Journal D. ***2005****, 34, 83–88.*

[7] S. R. M. D.J. Harding, and T.R. Walsh Chemical Physics Letters. ***2009****, 469, 31–34.*

[8] M. A. B. Matthew A. Addicoat, Brian Yates, Gregory F. Metha Journal of Computational Chemistry. ***2007****, 29, 1498-1506.*

[9] S. d. G. Garold Murdachaew, Giacinto Scoles J. Chem. Phys. A. ***2008****, 112, 9993–10005.*

[10] Mark B. Knickelbein Annu. Rev. Phys. Chem. ***1999****, 50, 79-115*

[11] Gaussian 03, Revision D.01,M. J. Frisch, G. W. Trucks, H. B. Schlegel, G. E. Scuseria, M. A. Robb, J. R. Cheeseman, J. A. Montgomery, Jr., T. Vreven, K. N. Kudin, J. C. Burant, J. M. Millam, S. S. Iyengar, J. Tomasi, V. Barone, B. Mennucci, M. Cossi, G. Scalmani, N. Rega, G. A. Petersson, H. Nakatsuji, M. Hada, M. Ehara, K. Toyota, R. Fukuda, J. Hasegawa, M. Ishida, T. Nakajima, Y. Honda, O. Kitao, H. Nakai, M. Klene, X. Li, J. E. Knox, H. P. Hratchian, J. B. Cross, V. Bakken, C. Adamo, J. Jaramillo, R. Gomperts, R. E. Stratmann, O. Yazyev, A. J. Austin, R. Cammi, C. Pomelli, J. W. Ochterski, P. Y. Ayala, K. Morokuma, G. A. Voth, P. Salvador, J. J. Dannenberg, V. G. Zakrzewski, S. Dapprich, A. D. Daniels, M. C. Strain, O. Farkas, D. K. Malick, A. D. Rabuck, K. Raghavachari, J. B. Foresman, J. V. Ortiz, Q. Cui, A. G. Baboul, S. Clifford, J. Cioslowski, B. B. Stefanov, G. Liu, A. Liashenko, P. Piskorz, I. Komaromi, R. L. Martin, D. J. Fox, T. Keith, M. A. Al-Laham, C. Y. Peng, A. Nanayakkara, M. Challacombe, P. M. W. Gill, B. Johnson, W. Chen, M. W. Wong, C. Gonzalez, and J. A. Pople, Gaussian, Inc., Wallingford CT, 2004.